Biogeosciences Discuss., 10, 7989–8025, 2013
www.biogeosciences-discuss.net/10/7989/2013/
doi:10.5194/bgd-10-7989-2013

Biogeosciences Discussions
Open Access

The calcareous nannofossil *Prinsiosphaera* achieved rock-forming abundances in the latest Triassic of western Tethys: consequences for the δ^{13}C of bulk carbonate

N. Preto[1,2], C. Agnini[1,3], M. Rigo[1,3], M. Sprovieri[4], and H. Westphal[2]

[1]Department of Geosciences, University of Padova, Via Gradenigo 6, 35131 Padova, Italy
[2]Leibniz Center for Marine Tropical Ecology, Bremen, Germany
[3]IGG-CNR, Padova, Italy
[4]IAMC-CNR Torretta Granitola, Trapani, Italy

Received: 4 April 2013 – Accepted: 16 April 2013 – Published: 14 May 2013

Correspondence to: N. Preto (nereo.preto@unipd.it)

Published by Copernicus Publications on behalf of the European Geosciences Union.

Abstract

The onset of pelagic biomineralization marked a milestone in the history of the long term inorganic carbon cycle: as soon as calcareous nannofossils became major limestone producers, the pH and supersaturation state of the global ocean were stabilized (the so-called Mid Mesozoic Revolution). But although it is known that calcareous nannofossils were abundant already by the end of the Triassic, no estimates exist on their contribution to hemipelagic carbonate sedimentation. With this work, we estimate the volume proportion of *Prinsiosphaera*, the dominant Late Triassic calcareous nannofossil, in hemipelagic and pelagic carbonates of western Tethys. The investigated Upper Triassic lime mudstones are composed essentially of microspar and tests of calcareous nannofossils, plus minor bioclasts. *Prinsiosphaera* became a significant component of lime mudstones since the late Norian, and was contributing up to ca. 60 % of the carbonate by the late Rhaetian in periplatform environments with hemipelagic sedimentation. The increasing proportion of *Prinsiosphaera* in upper Rhaetian hemipelagic lime mudstones is paralleled by a increase of the δ^{13}C of bulk carbonate. We interpreted this isotopic trend as related to the diagenesis of microspar, which incorporated respired organic carbon with a low δ^{13}C when it formed during shallow burial. As the proportion of nannofossil tests increased, the contribution of microspar with low δ^{13}C diminished, determining the isotopic trend. We suggest that a similar diagenetic effect may be observed in many Mesozoic limestones with a significant, but not yet dominant, proportion of calcareous plankton.

1 Introduction

Calcareous nannofossils have contributed significantly to pelagic sedimentation starting in the Late Triassic (Bellanca et al., 1995; Bralower et al., 1991; Bown, 1998, 2004; Gardin et al., 2012; Preto et al., 2013). The spreading of calcareous nannofossils had a major consequence on seawater chemistry, and on the long-term carbon cycle.

BGD
10, 7989–8025, 2013

Before pelagic biomineralization by calcareous nannofossils, carbon was sequestrated, in the form of calcium carbonate, only in platform areas, i.e., in areally limited portions of the global ocean. This implied a poor stabilization of carbonate species concentrations in seawater and, consequently, a variable seawater pH before the Triassic. An ocean in this state is, according to Zeebe and Westbroeck (2003), in "Neritan" mode. From the Jurassic on, precipitation of carbonates occurred both on platforms and in open oceans, in the form of calcitic tests of planktonic organisms (nannoliths, coccoliths, calcareous dinocysts, and, later on, planktonic foraminifers). An ocean in this state buffers the carbonic acid and the products of its dissociation more efficiently, resulting on a more stable seawater pH through geological times. It is called an ocean in "Cretan" mode (Zeebe and Westbroeck, 2003), and is similar, for what the carbonate chemistry is concerned, to the modern oceans. Clearly, the switch from the "Neritan" to the "Cretan" mode was a milestone in the evolution of ocean chemistry, and was thus baptized the "Mid Mesozoic Revolution" (Ridgwell, 2005).

But while the importance of this event is widely recognized, its temporal allocation is still vague. Ridgwell (2005) dates this event to sometime within the Jurassic, although with a high degree of uncertainty. However, it is usually understood that abundant calcareous nannofossils first appear in the Late Triassic (e.g., Bown, 1998; Erba, 2004; Furin et al., 2006).

Calcareous nannofossils were firstly described from the hemipelagic carbonates of the Tethys realm by Di Nocera and Scandone (1977) and then by Bellanca et al. (1993; 1995). These authors mostly illustrated unidentified calcispheres, which structure and diagenetic alteration was subsequently illustrated by Preto et al. (2013). Preto et al. (2012) then illustrates coccoliths and nannoliths from Pizzo Mondello in Sicily. In this locality *Prinsiosphaera* is abundant in the Rhaetian, with other calcareous planktonic forms (coccoliths and calcareous dinocysts) being largely subordinated. A Lower Jurassic (Pliensbachian) portion of the section instead yielded a rich coccolith flora and abundant calcispheres.

BGD
10, 7989–8025, 2013

Gardin et al. (2012) attempted to pin down precisely the first (common) occurrence of key Late Triassic nannofossil taxa as *Prinsiosphaera* and "coccolithophores". These taxa apparently become common only from the latest Sevatian (Upper Norian), i.e., much later than Bralower et al. (1991) suggested for ODP sites 759–761 and 764 on the Wombat Plateau offshore NW Australia. The study of Gardin et al. (2012) is based on condensed successions of the Northern Calcareous Alps in Austria and for the first time provides semi-quantitative estimation of calcareous nannofossil abundances in the Triassic, tightly constrained by conodont biostratigraphy. The quantification approach followed by Gardin et al., however, can only identify trends in nannofossil abundances, but give little information on the volume contribution of nannofossils to carbonate sedimentation. Preto et al. (2013) showed that "calcispheres" of uncertain taxonomic affinity become significant components of limestone from the base of the Upper Carnian, but their contribution to deep-water carbonate sedimentation is hard to quantify due to strong epitaxial calcite overgrowth.

In this contribution, we examine the distribution of the most common Late Triassic nannolith, *Prinsiosphaera*, in selected successions of the Southern Apennines and Sicily. The occurrence of common *Prinsiosphaera* in Sicily was documented by Preto et al. (2012). Our aim is to provide a quantification of nannofossils contribution to pelagic and hemipelagic carbonates. This study should thus be considered complementary to that of Gardin et al. (2012), both in terms of methods and because of the different paleogeographical position of the studied successions.

Analyses of the carbon stable isotope composition of bulk carbonate ($\delta^{13}C_{carb}$) were also performed, in order to identify possible correlations between nannofossil abundance and perturbations of the global carbon cycle. The effect of diagenesis was assessed with a combination of geochemical data and petrographic observations.

2 Geological setting

For this study, western Tethysian hemipelagic to pelagic carbonates and siliceous carbonates from the basinal domains of the Southern Apennines (Lagonegro Basin) and Sicily (Sicanian Basin) were sampled in two representative stratigraphic sections (Fig. 1) that apparently correlate with the increase in abundance of *Prinsiosphaera* observed in the late Norian by Gardin and co-authors (2012). The Norian facies are similar in the two areas: nodular cherty limestones with calcified radiolarian molds and thin-shelled bivalves. However, significant differences in the sedimentation between the Lagonegro and Sicanian basins are observed in the Late Norian and Rhaetian (latest Triassic), which is our interval of interest. We shall thus describe the typical succession of the two basins separately, also providing the current biostratigraphies.

2.1 Pizzo Mondello section in the Sicanian Basin

A periplatform carbonate succession of late Carnian to Jurassic age, belonging to the Sicanian Basin, crops out at Pizzo Mondello in central Sicily (Di Stefano, 1990; Gullo, 1996) (Fig. 1). Its lower portion is exposed on the walls of an abandoned quarry and was proposed as type section for the Global Boundary Stratotype Section and Point (GSSP) of the Norian (e.g., Muttoni et al., 2004; Balini et al., 2012; Mazza et al., 2012). The upper part is not similarly well exposed, but large intervals of the late Norian to Early Jurassic succession can be logged and sampled (Gullo, 1996; Mazza et al., 2012; Preto et al., 2012), and there is no evidence of discontinuities between the measured tracts of the section. For this study, we focused on the late Norian, Rhaetian and Early Jurassic portions of the succession (Fig. 2), which are well constrained by conodont biostratigraphy (Mazza et al., 2010, 2012), calcareous nannofossils and radiolarians (Preto et al., 2012). In this interval, the succession is comprised of chert-poor, cream to whitish nodular limestones, passing upward to whitish porous plane-bedded limestones (chalks). Greenish clay interlayers occur, but are rare and thin (about 1 cm): the succession is thus nearly completely carbonate.

2.2 Pignola–Abriola section in the Lagonegro Basin

The Carnian and Norian of the Lagonegro Basin (Fig. 1) are comprised of a thick succession of nodular limestones with chert nodules and beds, rich in radiolarian molds and thin-shelled bivalves mainly assignable to the genus *Halobia* (e.g., Scandone, 1967; Rigo et al., 2005, 2012a). Starting from the upper Norian (Sevatian) and continuing into the Rhaetian, the succession gradually becomes richer in shales and radiolarites through a ca. 30–40 m thick transitional interval (Amodeo, 1999; Passeri et al., 2005; Rigo et al., 2005, 2012a). The base of this transitional interval is marked by a ca. 3 m thick red shale horizon, dated to the late Norian *Mockina bidentata* conodont biochronozone (Rigo et al., 2005, 2012a). A radiolaritic succession of late Rhaetian to Late Jurassic age follows. The transition from deep-water carbonate sedimentation to shale-radiolarites that occurs basinwide in the late Norian-Rhaetian interval is interpreted as the deepening of the basin below the Carbonate Compensation Depth (e.g., Amodeo, 1999; Passeri et al., 2005; Giordano et al., 2011).

The studied succession at Pignola–Abriola (Fig. 3) encompasses most of the transitional interval above the basal red shale horizon, which is not documented, and the very base of the overlying shales and radiolarites. Conodont and radiolarian biostratigraphies constrain the succession to the late Norian–Rhaetian interval (Bazzucchi et al., 2005; Rigo et al., 2005, 2012a; Giordano et al., 2010).

3 Materials and methods

The proportion of *Prinsiosphaera* in the hemipelagic carbonates of this study was evaluated via point-counting of SEM images. The use of thin sections was excluded, because *Prinsiosphaera* can break down into single elements (scales or calcite plates) about 1 µm large that could not be seen under the optical microscope, not even in ultrathin sections (e.g., Erba and Tremolada, 2004).

Sixty-three samples of lime mudstone, silicified lime mudstone and intraclastic grainstone and breccia were prepared from Pignola–Abriola (Lagonegro Basin in the southern Apennines), while the 47 samples from Pizzo Mondello were all lime mudstone. Of the 63 samples from the Lagonegro Basin, only 20 were preserved well enough to allow point counting. The most common diagenetic alteration that made impossible to perform significant point counting was silicification (Fig. 4).

All samples were cut in blocks of ca. 5 × 5 mm, polished with borcarbid powder (500 and then 800 mesh per inch), etched for 20–30 s in 0.3 % hydrochloric acid, cleaned shortly in a ultrasonic bath, rinsed with deionized (Millipore) water, dried and gold coated. SEM images were taken at high magnification (ca. 2000 × to 3000 × and higher) with the Zeiss supra 40 of the Geowissenshaften, University of Bremen. Etching was necessary to highlight crystal boundaries (Preto et al., 2013).

Point-counting was performed by superimposing a regular grid of 28 columns and 19 rows (making up for 532 cross points) to SEM images (Fig. 5a–e). The grid spacing was chosen as to be larger than a single scale of *Prinsiosphaera*. A minimum of 2 up to 8 frames per sample were point counted, equaling 1064 to 4256 points counted per sample. This preparation ensured that estimations were made on a substantially flat surface.

Stable isotope analyses were performed on carbonate powders obtained with a dental drill from clean limestone surfaces, and carried out in two phases, first with Kiel and Bremen type Finnigan MAT mass spectrometers, reacting powders with H_3PO_4, at MARUM (University of Bremen), then by automated continuous flow carbonate preparation GasBenchII device (Spötl and Vennemann, 2003) and ThermoElectron Delta Plus XP mass spectrometer at the IAMC-CNR (Trapani, Italy) isotope geochemistry laboratory.

No systematic bias could be recognized between samples from the same sections, and ran in different laboratories. Care was taken to avoid late fractures, but it was impossible to separate calcareous nannofossils from their microsparitic matrix.

BGD

10, 7989–8025, 2013

4 Results

4.1 SEM petrology of nannofossil-bearing limestones

The samples chosen for this study come from well-bedded lime mudstones and wackestones, with the exception of one sample from Pignola–Abriola, from a m-scale calciturbidite bed. In this case, the microfacies and calcareous nannofossil abundance are referred to the reworked lime mudstone lithoclasts that make up the coarse portion of the calciturbidite.

In all samples, carbonates are given by an admixture of relatively large (5–15 µm on average) pitted microspar crystals and small (1 µm or less) platy calcite crystals (Figs. 5, 6). The latter are interpreted as elements of the calcareous nannofossils *Prinsiosphaera*, which can break down in loose scales (Fig. 5c, g; 6a). Often, however, these micron-scale platy calcite crystals or scales are still connected to form stacked groups of calcite plates and eventually spherical, solid nannoliths or "calcispheres" l.s. assignable to *Prinsiosphaera* (Fig. 6).

Microspar crystals may vary in dimensions between samples, and are generally larger when *Prinsiosphaera* is scarce. In the Rhaetian samples of Pizzo Mondello, where calcareous nannofossils often reach > 50 % of the rock volume, microspar crystals are mostly < 10 µm in diameter (Fig. 5e). The preservation of complete specimens of *Prinsiosphaera* is, however, not related to the dimension of microspar crystals: complete "calcispheres" are in fact found irrespective of their abundance or microspar crystal dimensions, and samples with abundant *Prinsiosphaera* and microspar < 10 µm may be mostly formed by fragmented "calcispheres". Scales of broken *Prinsiosphaera* are often engulfed by microspar crystals (Fig. 5).

Isolated dolomite rhombohedrons may also occur in samples from both sections (Fig. 4), similar to those described by Bellanca et al. (1995). Dolomite only constitutes a minor component of the rock volume, and was only rarely framed in the SEM images used for volume estimation of calcareous nannofossils.

Silicification is common at Pignola–Abriola (Fig. 4, 5j, 6g, j). Patches of amorphous silica or of unidentified silica minerals stick out on prepared SEM samples, because they are unaffected by etching. The proportion of sample that was silicified may vary from a few % to nearly all the rock volume (Fig. 4). Generally, point counting was still possible with a proportion of silica up to ca. 25 %. Silica do not appear to substitute the small calcite crystals of *Prinsiosphaera*, instead, it occupies intracrystalline spaces. Spaces that are normally occupied by microspar in other samples may be taken over by silica in silicified samples (Fig. 4c, d).

4.2 Calcareous nannofossils of the Sicanian and Lagonegro basins

The dominant calcareous nannofossil in the two examined sections is by far *Prinsiosphaera*. Other calcareous nannofossil taxa such as thoracospherids (Fig. 6b) do not contribute substantially to hemipelagic carbonate sedimentation in the Triassic, while the Jurassic assemblages of Pizzo Mondello are fairly diverse (Preto et al., 2012).

Prinsiosphaera is a still enigmatic nannolith, which features are strongly influenced by diagenetic alteration (Bralower et al., 1991). Its inner part is made of piles of micron-size scales that describe a full sphere. This inner part is the most easily preserved and was these micron-size scales that were recognized and point-counted in this study (Fig. 6). Differently from older calcispheres that tend to develop an epitaxial overgrowth (Gardin et al., 2012; Preto et al., 2013), *Prinsiosphaera* is always easy to tell from the surrounding sediment. However, spheres were found to break down easily, and scales are thus often found disarticulated in a microspar matrix (Figs. 5c, g, 6a). Also in these cases, the distinction between scales of *Prinsiosphaera* and small crystals of the matrix is rarely equivocal, as epitaxial overgrowths never occur.

4.3 Distribution of *Prinsiosphaera*

The first *Prinsiosphaera* we documented at Pizzo Mondello is within the *Mockina bidentata* conodont Zone, i.e., in the uppermost Norian (Fig. 2; Table 1). At Pignola–Abriola, the first *Prinsiosphaera* is observed immediately above a dolomitized interval present in the lower part of the succession within the upper Norian *Mockina bidentata* conodont Zone (Fig. 3; Table 2).

Prinsiosphaera is overall more common at Pizzo Mondello, where its abundance in limestones reaches 50–60 % by the late Rhaetian, in the *Misikella ultima* conodont Zone. Because of the high proportion of calcareous nannofossils with respect to carbonate constituents of the rock and incomplete cementation, the Rhaetian limestones of Pizzo Mondello (Portella Gebbia Limestone) are in fact chalks. The uppermost few meters of the Portella Gebbia Limestone cropping out in the Pizzo Mondello section belong to the Lower Jurassic (Pliensbachian; Preto et al., 2012). These limestones contain abundant calcareous nannofossils, constituting ca. 20–40 % of the rock volume.

At Pignola–Abriola, limestones are alternated to dominant shales, silicified claystones and cherts and thus constitute only a minor part of the rock volume. Furthermore, the amount of carbonate produced by calcareous nannofossils is proportionally minor within limestones, ranging between 2.5 and 15 % (Fig. 3; Table 2). A trend of increasing nannofossil abundance is again observed in the Rhaetian, within the *Misikella ultima* conodont Zone, where *Prinsiosphaera* constitutes up to 12–13 % of carbonate volume.

4.4 Carbon isotope composition of carbonate

The stable isotope composition of carbonate (Tables 3, 4) shows different values in the two analyzed sections, with a mean of $\delta^{13}C = 1.71 \pm 0.70$ ‰, $\delta^{18}O = -0.22 \pm 0.60$ ‰ at Pizzo Mondello and $\delta^{13}C = 1.00 \pm 1.00$ ‰, $\delta^{18}O = -3.10 \pm 1.84$ ‰ at Pignola–Abriola. The stable isotope composition of samples from Pizzo Mondello is within the range of seawater $\delta^{13}C$ estimated by Korte et al. (2005) for the Rhaetian (ca. 1 to 2.5 ‰), and in agreement with results of stable isotopic analyses on unaltered brachiopod shells from the Rhaetian of the Northern Calcareous Alps (Mette et al., 2012).

The $\delta^{13}C$ and $\delta^{18}O$ are strongly correlated at Pignola–Abriola, while only a small and negative correlation coefficient is found at Pizzo Mondello (Fig. 7). A few samples from

BGD
10, 7989–8025, 2013

Pignola–Abriola were sampled on a thick bed of coarse calciturbidite and exhibit the highest $\delta^{13}C$ values. All of these values are necessarily derived from bulk carbonate samples, which include both calcareous nannofossils and microspar. Contributions of minor carbonate components, as dolomite crystals or unidentified macrofossils, can be neglected on the base of petrographic observations.

A decrease of the $\delta^{13}C_{carb}$, reaching to the absolute minimum value recorded in the Pignola–Abriola section, nearly corresponds to the Norian/Rhaetian boundary. This stratigraphic interval is not exposed at Pizzo Mondello where, however, the lowest $\delta^{13}C_{carb}$ values are recorded at about the 29 m level in the highest outcropping beds belonging to *Misikella hernsteini–Paragondolella andrusovi* conodont zone (the youngest of the Norian). The base of the Rhaetian is thus generally associated with a rising trend of the $\delta^{13}C_{carb}$ values, which is best recorded at Pignola–Abriola. Interestingly, the contribution of calcareous nannofossils to carbonate production is also rising during the basal part of the Rhaetian in both sections (Fig. 2). More specifically, $\delta^{13}C_{carb}$ was found to be positively correlated with the content of calcareous nannofossils in both sections (Fig. 8).

5 Discussion

5.1 Contribution of calcareous nannofossils to hemipelagic carbonate sedimentation in Western Tethys

In our Triassic samples, nearly all calcareous nannofossils are assignable to *Prinsiosphaera*. The volume contribution of calcareous nannofossils becomes detectable starting from the upper Norian portion of the Pizzo Mondello section, within the Sevatian substage, a few meters below the last occurrence of the conodont *Mockina bidentata* and the first occurrence of *Misikella hernsteini*. The methods used in this study are not easily comparable to standard calcareous nannofossil counts of biostratigraphic investigations, which consist of semiquantitative counting performed on smear slides.

However, our data are roughly in agreement with the first abundant occurrence of nannoliths and coccoliths in Tethys in the late Norian, according to Gardin et al. (2012). This horizon is included, at Pignola–Abriola, within the basal interval affected by dolomitization and the first samples analyzed already contain a rather high proportion of nannofossils, > 10 %.

Afterward, the volume proportion of calcareous nannofossils increases, reaching 64 % by the late Rhaetian at Pizzo Mondello. In this locality, probably due to the high content of low-Mg calcite nannofossils and consequent paucity of metastable carbonate that could reprecipitate as microspar cement during diagenesis, upper Rhaetian and Jurassic lime mudstones retained high microporosity and are thus true chalk. The highest nannofossil abundances are reached in the late Rhaetian. Five Jurassic (Pliensbachian) samples show lower average volume contribution by calcareous nannofossils of 28 %.

It is interesting to compare the contribution of *Prinsiosphaera* in the two localities, keeping in mind that the facies of Pizzo Mondello are overall closer to a coastline, and probably shallower, than those of Pignola–Abriola (Rigo et al., 2012b). The Lagonegro Basin fell below the Carbonate Compensation Depth near the Triassic/Jurassic boundary, while Pizzo Mondello always remained above it. At Pignola–Abriola, the passage below the CCD is documented at the base of Jurassic radiolarites of the Scisti Silicei formation, at the top of the Pignola–Abriola section.

Prinsiosphaera is the dominant component of upper Rhaetian sediments at Pizzo Mondello but remains only a minor contributor in the more distal Pignola–Abriola section (Fig. 9). Moreover, the limestone beds are diluted by a high proportion of siliceous and clay beds at Pignola–Abriola, while the coeval succession of Pizzo Mondello is practically all limestone. We could not detect any obvious difference in preservation of nannofossils between the two localities. Specimens of *Prinsiosphaera* are always preserved as full spheres or isolated scales, but, for instance, there is no sign of a reduction of the volume of spheres due to dissolution. We thus assume that the difference in abundance between the two sections reflects a different origi-

BGD
10, 7989–8025, 2013

nal abundance of this nannolith. *Prinsiosphaera* was apparently more common in the shallower (proximal) periplatform basins of Sicily than in the more open marine setting of the Lagonegro Basin.

The main observation is, however, that calcareous nannofossils were a primary component of hemipelagic (or pelagic) carbonates during the latest Triassic. At that time, *Prinsiosphaera* must have played already a role in stabilizing the carbon cycle and thus in triggering the transition from a "Neritan" to a "Cretan" ocean (Zeebe and Westbroeck, 2003). This crucial event of the global carbon cycle, known as the "Mid Mesozoic Revolution" (Ridgwell, 2005), may thus date back to the end of the Late Triassic. The success of *Prinsiosphaera* as planktonic carbonate producer was however ephemeral: the Triassic/Jurassic mass extinction severely hit marine carbonate-secreting organisms, including *Prinsiosphaera* (Clémence et al., 2010), and calcareous nannofossils started over with a prolonged recovery. At Pizzo Mondello, the proportion of carbonate produced by calcareous nannofossils in the Pliensbachian, some 10 Myrs after the Triassic/Jurassic extinction, was not yet as high as it was at the end of the Triassic.

5.2 Interpretation of δ^{13}C values: admixture of seawater and marine burial diagenetic signals

The carbon isotope data of Pignola–Abriola show a negative excursion close to the Norian/Rhaetian boundary, followed by an increase of the $\delta^{13}C_{carb}$ during the Rhaetian (Fig. 3, 9). This pattern is not in contradiction with the incomplete isotopic record of Pizzo Mondello (Fig. 2). A negative excursion close to the Norian/Rhaetian boundary is also observed in the organic carbon isotope record of British Columbia (Sephton et al., 2002), and the following $\delta^{13}C_{carb}$ rise seems to be documented by Mette et al. (2012) in the Kössen Beds of the Northern Calcareous Alps. It is thus tempting to correlate these patterns in carbon isotope records from disparate regions and attribute them to a common climatic event. Our understanding of the petrography of limestones from the Lagonegro and Sicanian basins, however, suggests that this is not the case for the $\delta^{13}C_{carb}$ record of these sections.

BGD
10, 7989–8025, 2013

The $\delta^{13}C$ of bulk lime mudstone ($\delta^{13}C_{carb}$) is covariant with nannofossil abundance in both sections (Fig. 8). We propose that this reflects the admixture of carbonate from nannofossils, which carries the essentially unaltered carbon isotope composition of sea-surface waters, with carbonate of the microspar, which instead also incorporated respired organic carbon during shallow burial, when miscrospar crystals precipitated.

Microspar forms during shallow burial as the metastable aragonite dissolves and reprecipitates as low-Mg calcite. This process is well documented on the periplatform carbonates off Great Bahama Bank (Lasemi and Sandberg, 1984; Munnecke et al., 1997; Westphal, 2006) and was then recognized in numerous Phanerozoic deep-water limestone successions as, among others, the Silurian of Gotland (Munnecke et al., 1997), the upper Triassic of Southern Italy (Preto et al., 2009, 2013), the upper Jurassic of southern Germany (Munnecke and Westphal, 2004; Munnecke et al., 2008).

Within the periplatform carbonate sediments of the Bahamas, microspar was found and described in detail at depths of ca. 500 m downcore (Munnecke et al., 1997) and retains the carbon isotope signature of seawater (Melim et al., 1995, 2001). This was interpreted as the product of dissolution of aragonite and immediate reprecipitation of calcite in pore waters which composition was not altered with respect to the initial seawater. Aragonite is formed in shallow water environments of the Great Bahama Bank platform top, and is then exported in surrounding periplatform successions by processes as density cascading (Wilson and Roberts, 1995). Since aragonite derives from platforms, while calcite derives from tests of planktonic organisms (coccolitophorides and planktonic foraminifera), the aragonite/calcite ratio is a measure of platform-derived sediment in these environments (e.g., Droxler and Schlager, 1985; Reijmer et al., 1988; Schlager et al., 1994). Carbonate sediment comes either from the carbonate platform or from the photic zone of the open ocean, thus, in the periplatform deposits of Bahamas the carbon isotope composition of the original sediments is inherited fully from shallow waters.

The sedimentation environment of the Lagonegro Basin and Sicanian Basin should not have been different, especially during the Late Triassic, when calcareous nannofossils existed in rock-forming amounts (Preto et al., 2012, 2013; Rigo et al., 2012a). There is evidence of nearby carbonate platforms exporting carbonate into basins, both for the Lagonegro Basin (e.g., Miconnet et al., 1983; Bertinelli et al., 2005; Passeri et al., 2005; Rigo et al., 2007) and Pizzo Mondello (Rigo et al., 2012b). We can thus assume that the microsparitic component associated with calcareous nannofossils derived, in both sections, from shallow-water aragonite sediment, dissolved and reprecipitated in the marine burial diagenetic environment (Melim et al., 1995).

If the microspar component of the lime mudstone incorporated light carbon from the respiration of organic matter while forming during shallow burial, this would have lowered its δ^{13}C and could explain the correlation between the content of calcareous nannofossils and the carbon isotope composition of limestones. Only calcareous nannofossils retained a pristine seawater δ^{13}C, while the bulk carbonate registered the admixture of a pristine carbon isotope signal of seawater (carried by calcareous nannoplankton) and a δ^{13}C lowered by respired carbon (carried by microspar). The lower δ^{13}C and δ^{18}O values of Pignola–Abriola, which are also strongly correlated, are explained by a higher proportion of incorporated organic carbon and reprecipitation that was completed at higher depths, and thus higher burial temperatures, than at Pizzo Mondello. Higher burial temperatures, which are also suggested by a higher Color Alteration Index (CAI) of conodonts at Pignola–Abriola with respect to Pizzo Mondello (Giordano et al., 2010; Rigo et al., 2012b), drove the δ^{18}O to lower values (e.g., Allan and Matthews, 1982; Marshall, 1992).

In short, the $\delta^{13}C_{carb}$ record of Pizzo Mondello and Pignola–Abriola mostly documents diagenetic processes. This does not exclude that a carbon isotope excursion exists at the Norian/Rhaetian boundary, however, bulk carbonate is an inadequate substrate to prove it, and in fact no excursion is registered at the Norian/Rhaetian boundary by the $\delta^{13}C_{carb}$ of other stratigraphic sections (e.g., Ward et al., 2004; Krystyn et al., 2007; see also Fig. 9). The stable isotope composition of bulk carbonate could only have been interpreted as a seawater signal if carbonate precipitation was demonstrated to occur at very shallow depth in the sediment column, close to the water-sediment

BGD
10, 7989–8025, 2013

interface. Lime mudstones made of coarse (10–30 µm) microspar should be instead considered with caution (Preto et al., 2009), as microspar forms during burial and most probably also incorporates a burial diagenetic carbon isotope signal. More generally, the $\delta^{13}C_{carb}$ should not be considered a proxy for the $\delta^{13}C$ of seawater, unless a solid petrographic study is provided that proves this assumption.

The coincidence of the negative excursion in the $\delta^{13}C_{carb}$ of Pignola–Abriola and in the $\delta^{13}C$ of organic matter in British Columbia (Sephton et al., 2002) can be explained in many ways. A possibility is that a climatic perturbation at the Norian/Rhaetian boundary augmented the ocean primary productivity, and thus the exportation of organic matter to the sea floor. An initial higher content of organic matter would allow more of it to be preserved at the time of aragonite to calcite transformation during burial, and thus a higher availability of respired carbon that could be incorporated in the microspar. Alternatively, the carbon isotope excursion of British Columbia may be an artifact, or a product of diagenesis. This could only be determined by duplicating, in coeval stratigraphic successions, the $\delta^{13}C$ excursion on an adequate substrate: e.g., brachiopod or oyster shells screened for diagenetic alteration, organic matter of uniform composition or specific organic molecules.

Stable isotope records of Triassic successions based on bulk carbonate, as, to name a few, Payne et al. (2004), Horacek et al. (2007), Muttoni et al. (2004), Mazza et al., (2010) and, at least in part, Korte et al. (2005) should thus be interpreted with extreme caution, with an adequate discussion of diagenetic processes. Once the precipitation of carbonate in the pelagic realm becomes firmly established, instead, deep-water lime mudstones may be mostly made of calcareous plankton, and should retain the seawater $\delta^{13}C$ more easily. Our study shows that the Late Rhaetian *Misikella ultima* biochronozone is perhaps the first time of Earth history when this could have happened.

BGD
10, 7989–8025, 2013

6 Conclusions

Prinsiosphaera, an *incertae sedis* Late Triassic calcareous nannofossil forming characteristic solid "calcispheres", is a major contributor to deep-water carbonate sedimentation in Western Tethys, and can constitute up to 60 % ca. of the rock volume in hemipelagic lime-mudstones of latest Triassic (late Rhaetian) age. In the studied sections of Southern Italy, its first common occurrence in lime mudstones is dated to the late Norian (Late Triassic), within the *Mockina bidentata* conodont biochronozone.

Upper Rhaetian lime mudstones are constituted in significant proportion by *Prinsiosphaera* both in the Lagonegro and the Sicanian Basin sections (southern Italy). The latest Triassic was thus the first time in Earth history when calcareous plankton reached rock forming abundances, and the start-up of the so-called "Mid-Mesozoic Revolution" of Ridgwell (2005), when the long term carbon cycle in the oceans was permanently stabilized by the initiation of a pelagic carbonate factory.

The increase of calcareous nannofossils in the Late Triassic coincided with a positive shift of the $\delta^{13}C$ of bulk carbonate. However, this does not represent a pristine seawater isotopic signal but rather a diminishing contribution of microspar, which incorporated respired organic carbon during diagenesis, as the proportion of nannofossils increases. We suggest that a similar diagenetic influence should be observed in most Mesozoic isotope records from bulk carbonate, and could only be excluded by careful petrographic examinations.

Acknowledgements. Petra Witte (Geowissenshaften, Bremen), Monika Segl (MARUM, Bremen) and Sebastian Flotow (ZMT, Bremen) assisted in the labs. Stefano Borello (Padova) prepared most of the isotope samples.

Alda Nicora, Michele Mazza (Milano) and Guido Roghi (IGG-CNR Padova) helped in the field. Pietro Di Stefano gave insights on the stratigraphy and paleogeography of Sicily. This study was funded by the Alexander von Humboldt Foundation (to NP) and by the University of Padova (Progetto d'Ateneo CPDA090175/09 to MR) and by the MIUR (Prin 2008BEF5Z7_005 to MR).

References

Allan, J. R. and Matthews, R. K.: Isotope signatures associated with early meteoric diagenesis, Sedimentology, 29, 797–817, 1982.

Amodeo, F.: Il Triassico terminale – Giurassico del Bacino Lagonegrese, studi stratigrafici sugli Scisti Silicei della Basilicata (Italia Meridionale), Mémoirs de Géologie (Lousanne), 33, 1–121, 1999.

Balini, M., Krystyn, L., Levera, M., and Tripodo, A.: Late Carnian-early Norian ammonoids from the GSSP candidate section Pizzo Mondello (Sicani Mountains, Sicily), Riv. Ital. Paleontol. S., 118, 47–84, 2012.

Bazzucchi, P., Bertinelli, A., Ciarapica, G., Marcucci, M., Passeri, L., Rigo, M., and Roghi, G.: The Late Triassic–Jurassic stratigraphic succession of Pignola (Lagonegro-Molise Basin, southern Apennines, Italy, Boll. Soc. Geol. Ital., 124, 143–153, 2005.

Bellanca, A., Di Stefano, E., Di Stefano, P., Erba, E., Neri, R., and Pirini Radrizzani, C.: Ritrovamento di “Calcisfere” e nannofossili calcarei in terreni carnici della Sicilia, Paleopelagos, 3, 91–96, 1993.

Bellanca, A., Di Stefano, P., and Neri, R.: Sedimentology and isotope geochemistry of Carnian deep-water marl/limestone deposits from the Sicani Mountains, Sicily: environmental implications and evidence from planktonic source of lime mud, Palaeogeogr. Palaeoclimatol. Palaeoecol., 114, 111–129, 1995.

Bertinelli, A., Ciarapica, G., De Zanche, V., Marcucci, M., Mietto, P., Passeri, L., Rigo, M., and Roghi, G.: Stratigraphic evolution of the Triassic-Jurassic Sasso di Castalda succession (Lagonegro basin, southern Apennines, Italy), Boll. Soc. Geol. Ital., 124, 161–175, 2005.

Bown, P. R.: Calcareous Nannofossil Biostratigraphy, Kluwer Academic, Dordrecht, 1998.

Bown, P. R., Lees, J. A., and Young, J. R.: Calcareous nannoplankton evolution and diversity through time, in: Coccolithophores – from molecular processes to global impact, Springer Verlag, Berlin, 481–505, 2004.

Bralower, T. J., Bown, P. R., and Siesser, W. G.: Significance of Upper Triassic nannofossils from the Southern Hemisphere (ODP Leg 122, Wombat Plateau, N. W. Australia), Mar. Micropaleontol., 17, 119–154, 1991.

Clémence, M. E., Gardin, S., Bartolini, A., Paris, G., Beaumont, V., and Guex, J.: Bentho-planktonic evidence from the Austrian Alps for a decline in sea-surface carbonate production at the end of the Triassic, Swiss J. Geosci., 103, 293–315, 2010.

Di Nocera, S. and Scandone, P.: Triassic nannoplankton limestones of deep basin origin in the central mediterranean region, Palaeogeogr. Palaeoclimatol. Palaeoecol., 21, 101–111, 1977.
Di Stefano, P.: The Triassic of Sicily and the southern Appennines, Boll. Soc. Geol. Ital., 109, 21–37, 1990.
Di Stefano, P., Alessi, A, and Gullo, M.: Mesozoic and Paleogene megabreccias in southern Sicily: new data on the Triassic paleomargin of the Siculo-Tunisian Platform, Facies, 34, 101–122, 1996.
Droxler, A. W. and Schlager, W.: Glacial versus interglacial sedimentation rates and turbidite frequency in the Bahamas, Geology, 13, 799–802, 1985.
Erba, E.: Calcareous nannofossils and Mesozoic oceanic anoxic events, Mar. Micropaleontol., 52, 85–106, 2004.
Erba, E. and Tremolada, F.: Nannofossil carbonate fluxes during the early Cretaceous: Phytoplankton response to nitrification episodes, atmospheric CO_2, and anoxia, Paleoceanography, 19:PA1008, 1–18, 2004.
Furin, S., Preto, N., Rigo, M., Roghi, G., Gianolla, P., Crowley, J., and Bowring, S. A.: A high-precision U/Pb zircon age from the Triassic of Italy – implications for the Carnian rise of calcareous nannoplancton and dinosaurs, Geology, 34, 1009–1012, 2006.
Gardin, S., Krystyn, L., Richoz, S., Bartolini, A., and Galbrun, B.: Where and when the earliest coccolithophores?, Lethaia, 45, 507–523, 2012.
Giordano, N., Rigo, M., Ciarapica, G., and Bertinelli, A.: New biostratigraphical constraints for the Norian/Rhaetian boundary: data from Lagonegro Basin, southern Apennines, Italy, Lethaia, 43, 573–586, 2010.
Giordano, N., Ciarapica, G., Bertinelli, A., and Rigo, M.: The Norian-Rhaetian interval in two sections of the Lagonegro area: the transition from carbonate to siliceous deposition, Ital. J. Geosci., 130, 380–393, 2011.
Gullo, M.: Conodont biostratigraphy of uppermost Triassic deep-water calcilutites from Pizzo Mondello (Sicani Mountains): evidence for Rhaetian pelagites in Sicily, Palaeogeogr. Palaeoclimatol. Palaeoecol., 126, 309–323, 1996.
Korte, C., Kozur, H. W., and Veizer, J.: $\delta^{13}C$ and $\delta^{18}O$ values of Triassic brachiopods and carbonate rocks as proxies for coeval seawater and palaeotemperature, Palaeogeogr. Palaeoclimatol. Palaeoecol., 226, 287–306, 2005.

Kozur, H. and Mock, R.: New Middle Carnian and Rhaetian conodonts from Hungary and the Alps, stratigraphic importance and tectonic implications for the Buda Mountains and adjacent areas, Jb. Geol. Bundesanst., 134, 271–297, 1991.

Krystyn, L., Bouquerel, H., Kuerschner, W., Richoz, S., and Gallet, Y.: Proposal for a candidate GSSP for the base of the Rhaetian stage, New Mexico Museum of Natural History and Science Bulletin, 41, 189–199, 2007.

Horacek, M., Brandner, R., and Abart, R.: Carbon isotope record of the P/T boundary and the Lower Triassic in the Southern Alps: evidence for rapid changes in storage of organic carbon, Palaeogeogr. Palaeoclimatol. Palaeoecol., 252, 347–354, 2007.

Lasemi, Z. and Sandberg, P. A.: Transformation of aragonite-dominated lime muds to microcrystalline limestones, Geology, 12, 420–423, 1984.

Marshall, J. D.: Climatic and oceanographic isotopic signals from the carbonate rock record and their preservation, Geol. Mag., 129, 151–162, 1992.

Mazza, M., Furin, S., Spötl, C., and Rigo, M.: Generic turnovers of Carnian/Norian conodonts: climatic control or competition?, Palaeogeogr. Palaeoclimatol. Palaeoecol., 290, 120–137, 2010.

Mazza, M., Rigo, M., and Gullo, M.: Taxonomy and biostratigraphic record Upper Triassic conodonts of the Pizzo Mondello section (western Sicily, Italy), GSSP candidate for the base of the Norian, Riv. Ital. Paleontol. S., 118, 85–130, 2012.

Melim, L. A., Swart, P. K., and Maliva, R. G.: Meteoric-like fabrics forming in marine waters: implications for the use of petrography to identify diagenetic environments, Geology, 23, 755–758, 1995.

Melim, L. A., Swart, P. K., and Maliva, R. G.: Meteoric and marine-burial diagenesis in the subsurface of Great Bahama Bank, SEPM Spec. P., 70, 137–161, 2001.

Mette, W., Elsler, A., and Korte, C.: Palaeoenvironmental changes in the Late Triassic (Rhaetian) of the northern Calcareous Alps: clues from stable isotopes and microfossils, Palaeogeogr. Palaeoclimatol. Palaeoecol., 350–352, 62–72, 2012.

Miconnet, P., Ciarapica, G., and Zaninetti, L.: Faune a Foraminifères du Trias supérieur d'affinité sud-Tethysienne dans l'Apennin méridional (Bassin de Lagonegro, province de Potenza, Italie), comparaison avec l'Apennin septentrional, Rev. Paléobiol., 2, 131–147, 1983.

Munnecke, A. and Westphal, H.: Shallow-water aragonite recorded in bundles of limestone-marl alternations – the upper Jurassic of SW Germany, Sediment Geol., 164, 191–202, 2004.

Discussion Paper | Discussion Paper | Discussion Paper | Discussion Paper |

Munnecke, A., Westphal, H., Reijmer, J. J. G., and Samtleben, C.: Microspar development during early marine burial diagenesis: a comparison of Pliocene carbonates from the Bahamas with Silurian limestones from Gotland (Sweden), Sedimentology, 44, 977–990, 1997.

Munnecke, A., Westphal, H., and Kölbl-Ebert, M.: Diagenesis of plattenkalk: examples from the Solnhofen area (upper Jurassic, southern Germany), Sedimentology, 55, 1931–1946, 2008.

Muttoni, G., Kent, D. V., Olsen, P. E., Di Stefano, P., Lowrie, W., Bernasconi, S. M., and Hernandez, F. M.: Tethyan magnetostratigraphy from Pizzo Mondello (Sicily) and correlation to the Late Triassic Newark astrochronological polarity time scale, Geol. Soc. Am. Bull., 116, 1034–1058, 2004.

Passeri, L., Bertinelli, A., and Ciarapica, G.: Palaeogeographic meaning of the late Triassic–early Jurassic Lagonegro units, Boll. Soc. Geol. Ital., 124, 231–245, 2005.

Payne, J. L., Lehrmann, D. J., Wei, J., Orchard, M. J., Schrag, D. P., and Knoll, A. H.: Large perturbations of the carbon cycle during recovery from the End-Permian extinction, Science, 305, 506–509, 2004.

Preto, N., Spötl, C., and Guaiumi, C.: Evaluation of bulk carbonate δ^{13}C data from Triassic hemipelagites and the initial composition of carbonate mud, Sedimentology, 56, 1329–1345, 2009.

Preto, N., Rigo, M., Agnini, C., Bertinelli, A., Guaiumi, C., Borello, S., and Westphal, H.: Triassic and Jurassic calcareous nannofossils of the Pizzo Mondello section: a SEM study, Riv. Ital. Paleontol. S., 118, 131–141, 2012.

Preto, N., Willems, H., Guaiumi, C., and Westphal, H.: Onset of significant pelagic carbonate accumulation after the Carnian Pluvial Event (CPE) in the western Tethys, Facies, doi:10.1007/s10347-012-0338-9, 2013.

Reijmer, J. J. G., Schlager, W., and Droxler, A. W.: Site 632: Pliocene–Pleistocene sedimentation cycles in a Bahamian Basin, in: Proc. of the ODP Sci. Results, 166, edited by: Austin, J. A. J. and Schlager, W., 213–220, 1988.

Ridgwell, A.: A mid Mesozoic revolution in the regulation of ocean chemistry, Mar. Geol., 217, 339–357, 2005.

Rigo, M., De Zanche, V., Gianolla, P., Mietto, P., Preto, N., and Roghi, G.: Correlation of Upper Triassic sections throughout the Lagonegro Basin, Boll. Soc. Geol. Ital., 124, 293–300, 2005.

Rigo, M., Preto, N., Roghi, G., Tateo, F., and Mietto, P.: A CCD rise in the Carnian (upper Triassic) of western Tethys, deep-water equivalent of the Carnian Pluvial Event, Palaeogeogr. Palaeoclimatol. Palaeoecol., 246, 188–205, 2007.

BGD
10, 7989–8025, 2013

The calcareous nannofossil *Prinsiosphaera*

N. Preto et al.

Rigo, M., Preto, N., Franceschi, M., and Guaiumi, C.: Stratigraphy of the Carnian–Norian Calcari con Selce Formation in the Lagonegro Basin, southern Apennines, Riv. Ital. Paleontol. S., 118, 143–154, 2012a.

Rigo, M., Trotter, J., Preto, N., and Williams, I.: Isotopic evidence of late Triassic monsoonal upwelling in the northwestern Tethys, Geology, 40, 515–518, 2012b.

Scandone, P.: Studi di geologia lucana: la serie calcareo-silico- marnosa, Bollettino della Società dei Naturalisti di Napoli, 76, 1–175, 1967.

Schlager, W., Reijmer, J. J. G., and Droxler, A.: Highstand shedding of carbonate platforms, J. Sediment. Res., 64, 270–281, 1994.

Sephton, M. A., Amor, K., Franchi, I. A., Wignall, P. B., Newton, R., and Zonneveld, J- P.: Carbon and nitrogen isotope disturbances and an end-Norian (late Triassic) extinction event, Geology, 30, 1119–1122, 2002.

Spötl, C. and Vennemann, T. W.: Continuous-flow isotope ratio mass spectrometric analysis of carbonate minerals, Rapid Commun. Mass Spectrom., 17, 1004–1006, 2003.

Ward, P. D., Garrison, G. H., Haggart, J. W., Kring, D. A., and Beattie, M. J.: Isotopic evidence bearing on late Triassic extinction events, Queen Charlotte Islands, British Columbia, and implications for the duration and cause of the Triassic/Jurassic mass extinction, Earth Planet. Sci. Lett., 224, 589–600, 2004.

Westphal, H.:. Limestone-marl alternations as environmental archives and the role of early diagenesis: a critical review, Int. J. Earth Sci., 95, 947–961, 2006.

Wilson, P. A. and Roberts, H. H.: Density cascading – off-shelf sediment transport, evidence and implications, Bahama Banks, J. Sediment. Res., 65, 45–56, 1995.

Zeebe, R. E. and Westbroek, P.:. A simple model for the $CaCO_3$ saturation state of the ocean: the “Strangelove”, the “Neritan”, and the “Cretan” Ocean, Geochem. Geophy. Geosy., 4, 1–26, 2003.

Table 1. Nannofossil content of analyzed limestones at Pizzo Mondello. Stratigraphic heights (H) as in Fig. 2. Some limestones were sampled in poorly outcropping parts of the section that were located but not logged. Each point count of column 2 (Nannofossils) refer to a framed SEM image. The third column refers to the average of all images on which point counting was made for that sample.

H (m)	Nanno-fossils (% volume)	Average (% volume)	H (m)	Nanno-fossils (% volume)	Average (% volume)	H (m)	Nanno-fossils (% volume)	Average (% volume)	H (m)	Nanno-fossils (% volume)	Average (% volume)	H (m)	Nanno-fossils (% volume)	Average (% volume)
	Part 1		16.48	7.89	7.52	22.19	4.32	3.48	35.70	25.19	24.25	54.50	52.10	64.16
9.71	1.69	1.57		8.46			1.88			23.31			68.40	
	1.32			7.33			4.32		36.60	40.79	39.79		71.99	
	1.88			6.20			4.13			40.41		54.90	40.04	36.66
	0.94			7.52			2.63			38.16			33.27	
	1.32			7.71			3.57		37.50	28.76	28.70	55.40	67.10	55.60
	2.26		17.07	3.76	3.76	22.60	1.69	2.76		31.58			36.09	
10.01	1.88	2.36		3.95			0.19			25.75			62.03	
	1.69			5.26			1.50		38.55	42.29	40.79		48.68	
	3.38			3.76			5.64			39.29			64.10	
	3.38			3.57			5.26		39.75	46.43	29.68			
	1.88			2.82			2.26			47.56			**Part 4**	
	2.07			3.19		23.47	10.53	14.42		12.78		60.00	28.38	23.68
	2.26		17.47	4.51	5.49		17.86			16.73			18.98	
				2.82			18.05			17.48		62.70	36.28	33.18
	Part 2			8.83			15.04			41.73			30.07	
13.10	7.33	4.86		6.01			14.85			33.08		64.00	41.54	40.10
	5.26			5.26			16.17			38.53			38.91	
	5.26		17.70	8.65	7.52		8.46		40.25	27.63	27.16		39.85	
	1.69			8.49						26.69		65.10	25.19	24.82
	3.76			9.21			**Part 3**		41.85	41.54	32.71		24.44	
	5.83			6.58		31.50	35.53	20.93		30.26		66.00	17.10	18.92
13.39	2.63	4.18		5.26			14.29			26.32			19.55	
	4.13			5.45			12.97		42.25	63.91	55.55		20.11	
	5.07			9.02		32.50	30.64	28.57		47.18				
	4.70		19.95	1.69	2.68		26.50		52.05	39.29	44.84			
	5.45			2.44		33.50	27.26	23.37		50.38				
	3.95			3.01			23.50		52.55	30.64	25.75			
	3.57			3.57			19.36			20.86				
	3.95					34.50	27.44	28.20						
							28.95							

Table 2. Nannofossil content of analyzed limestones at Pignola–Abriola. Stratigraphic heights (H) as in Fig. 3. Each point count of column 2 (Nannofossils) refer to a framed SEM image. The third column refers to the average of all images on which point counting was made for that sample.

H (m)	Nannofossils (% volume)	Average (% volume)
19.50	17.48	15.13
	12.78	
21.25	8.46	10.02
	9.90	
	9.90	
	10.00	
	11.84	
23.70	13.53	14.45
	20.86	
	13.72	
	13.98	
	13.26	
	11.33	
24.20	6.01	8.36
	10.71	
25.60	5.45	4.37
	2.82	
	4.89	
	4.32	
	4.70	
	6.20	
	3.95	
	2.63	
28.10	8.08	9.31
	10.53	

H (m)	Nannofossils (% volume)	Average (% volume)
33.30	3.95	6.09
	7.52	
	3.95	
	5.83	
	6.39	
	3.57	
	7.14	
	10.34	
37.40	3.57	3.90
	3.95	
	4.70	
	3.38	
37.70	4.89	6.02
	7.14	
40.70	1.50	2.58
	3.57	
	2.63	
	2.63	
50.90	6.39	9.07
	5.45	
	8.83	
	7.71	
	10.90	
	9.02	
	11.09	
	13.16	

H (m)	Nannofossils (% volume)	Average (% volume)
51.80	2.26	1.69
	1.50	
	1.32	
52.10	5.64	6.06
	6.77	
	4.89	
	6.95	
52.50	2.26	3.64
	3.57	
	3.76	
	2.63	
	4.70	
	4.89	
54.90	3.95	4.51
	5.07	
57.20	15.04	11.00
	7.14	
	10.90	
	8.84	
	9.77	
	14.29	
57.30	4.89	7.43
	5.64	
	9.96	
	9.21	

H (m)	Nannofossils (% volume)	Average (% volume)
57.90	9.77	12.29
	15.79	
	16.54	
	5.83	
	13.53	
58.30	12.78	12.84
	14.10	
	16.35	
	9.77	
	13.35	
	11.09	
	12.41	
58.80	12.41	12.72
	17.48	
	11.65	
	12.22	
	10.15	
	12.41	

Table 3. Stable isotope composition of oxygen and carbon in limestones of the Pizzo Mondello Section. Stratigraphic heights (*H*) as in Fig. 2.

H (m)	$\delta^{18}O$	$\delta^{13}C$	*H* (m)	$\delta^{18}O$	$\delta^{13}C$	*H* (m)	$\delta^{18}O$	$\delta^{13}C$
	Part 1		19.20	0.14	1.59	38.55	−0.33	1.92
5.00	−0.61	2.21	19.95	0.18	1.55	39.25	−0.02	2.05
5.30	−0.79	1.95	20.50	−0.16	1.36	39.75	−0.30	2.04
6.02	−0.64	1.85	21.35	−0.09	1.18	40.25	−0.79	1.80
6.27	−0.26	1.67	22.19	−0.76	0.93	41.85	−0.16	2.13
6.90	−0.37	1.61	22.60	−0.64	1.30	42.25	−0.18	2.14
7.25	−1.02	1.76	23.47	0.18	1.41	44.35	−0.59	1.78
7.95	−0.68	1.77	24.00	−0.12	1.29	52.05	−0.37	1.85
8.47	−0.27	1.72	25.76	0.28	1.34	52.55	0.17	2.08
9.71	0.10	1.52	26.26	0.04	1.25	54.50	−0.59	2.10
10.01	−0.25	1.59	26.63	0.02	1.16	54.90	−0.35	2.16
			27.11	0.15	1.24	55.40	−0.14	2.15
	Part 2		27.41	−0.44	1.10			
12.00	0.07	1.49	28.30	0.00	0.93		**Part 4**	
12.60	−0.47	2.00	28.72	0.08	1.19	60.00	−0.20	2.29
13.10	−0.04	1.60	29.08	−0.16	1.27	62.70	0.01	2.12
13.39	−0.29	1.11				64.00	−0.37	2.07
13.80	−0.24	1.45		**Part 3**		65.10	−0.66	1.82
14.10	−0.20	1.50	35.00	−0.55	2.09			
14.30	−0.15	1.38	35.70	−0.04	1.99			
14.44	−0.22	1.72	36.10	−0.17	1.98			
15.73	−0.31	1.49	36.60	−0.42	1.99			
16.48	0.03	1.59	37.10	−0.41	1.93			
17.07	0.28	1.56	37.50	−0.22	1.87			
17.47	0.54	1.56	37.90	0.08	2.07			
17.70	0.10	1.50	38.20	−0.05	1.88			

BGD
10, 7989–8025, 2013

Table 4. Stable isotope composition of oxygen and carbon in limestones of the Pizzo Mondello Section. Stratigraphic heights (*H*) as in Fig. 3.

H (m)	$\delta^{18}O$	$\delta^{13}C$	*H* (m)	$\delta^{18}O$	$\delta^{13}C$	*H* (m)	$\delta^{18}O$	$\delta^{13}C$	*H* (m)	$\delta^{18}O$	$\delta^{13}C$	*H* (m)	$\delta^{18}O$	$\delta^{13}C$
18.31	−2.82	1.00	25.73	−2.33	1.40	34.60	−1.66	1.38	46.09	−4.94	0.64	54.28	−3.79	0.90
19.06	−3.60	−0.05	26.10	−2.02	1.58	37.13	−2.41	1.18	46.19	−5.51	0.47	54.61	−3.86	1.18
19.32	−4.29	−1.80	26.27	−1.96	1.50	37.34	−2.51	1.40	46.28	−4.37	−0.69	54.61	−3.61	0.86
19.52	−2.17	1.53	26.34	−2.04	1.52	37.55	−2.02	2.02	46.34	−3.81	0.32	54.75	−3.29	1.02
19.81	−4.57	0.31	26.49	−1.94	1.58	37.67	−2.99	1.40	46.61	−5.18	0.48	54.92	−2.30	1.59
20.06	−2.35	1.65	26.78	−2.85	1.29	38.53	−1.98	2.05	46.68	−3.44	0.68	55.17	−1.97	1.52
20.18	−3.76	0.10	26.99	−2.65	1.36	39.07	−2.17	2.07	46.77	−3.24	0.47	55.30	−2.91	1.20
20.59	−2.87	1.14	27.09	−2.56	1.29	39.16	−3.85	1.03	47.19	−3.30	0.36	55.40	−4.01	1.18
20.96	−2.30	1.23	27.26	−3.01	1.19	39.38	−2.80	1.30	47.35	−3.66	0.27	55.51	−3.63	1.09
21.30	−2.38	1.46	27.46	−2.27	1.28	40.29	−2.48	1.48	47.59	−4.01	−0.01	55.73	−4.08	1.06
21.36	−2.05	1.20	27.62	−2.12	1.14	40.75	−4.22	1.23	47.88	−3.85	0.13	55.73	−2.83	1.10
21.74	−2.47	1.07	27.95	−1.94	1.37	41.01	−4.85	0.52	48.03	−4.11	0.49	55.93	−3.38	0.99
21.83	−2.67	0.94	28.10	−1.94	1.42	41.11	−4.14	0.80	48.73	−3.19	0.94	56.25	−4.51	0.67
21.98	−2.66	0.92	28.17	−1.90	1.47	41.57	−4.52	0.79	48.86	−2.92	1.02	56.35	−4.43	0.92
22.12	−2.50	1.38	28.24	−2.72	1.09	42.06	−4.75	0.74	48.96	−4.25	0.43	56.47	−3.93	0.95
22.24	−3.29	1.08	28.48	−2.32	1.20	42.21	−3.67	0.66	49.13	−3.61	0.19	56.71	−3.10	1.09
22.45	−2.33	1.13	28.67	−2.34	1.24	42.27	−4.50	0.52	49.26	−4.59	0.34	56.90	−3.70	1.21
22.66	−2.22	1.27	28.87	−2.54	1.02	42.44	−2.66	1.23	49.26	−4.51	0.09	56.92	−3.27	1.12
23.03	−2.16	1.25	31.18	−2.44	0.99	42.65	−2.35	1.20	49.44	−4.21	0.05	57.17	−3.59	0.98
23.17	−1.40	1.56	31.71	−2.04	1.17	42.93	−2.96	1.42	49.90	−3.48	0.49	57.27	−4.19	1.26
23.54	−2.14	1.60	31.84	−2.31	1.17	43.17	−2.66	1.30	50.35	−3.00	0.88	57.64	−2.82	0.95
23.72	−4.35	0.64	32.30	−2.56	0.84	43.57	−3.68	1.22	50.35	−3.38	0.51	57.87	−3.96	1.26
23.72	−2.26	1.57	32.39	−2.20	0.98	43.91	−3.86	1.02	50.88	−2.52	1.05	58.02	−3.66	1.23
23.90	−3.54	1.22	32.59	−2.10	1.04	44.22	−2.80	1.19	50.88	−3.31	0.81	58.39	−4.50	1.15
24.06	−2.50	1.31	32.88	−1.91	1.31	44.37	−3.34	0.96	51.35	−3.08	1.02	58.57	−2.92	1.14
24.17	−2.53	1.42	33.30	−1.24	1.42	44.44	−4.59	0.58	51.85	−3.42	0.73	58.70	−2.58	1.41
24.32	−2.65	1.24	33.42	−2.29	1.16	44.53	−3.53	1.05	52.13	−3.00	0.74			
24.47	−3.82	1.26	33.51	−3.96	0.88	44.68	−4.14	0.02	52.45	−3.24	0.81			
24.82	−2.83	1.14	33.42	−1.85	1.44	44.79	−4.98	−0.22	52.78	−2.46	1.29			
25.00	−3.20	1.00	33.94	−1.88	1.50	45.03	−4.34	0.29	53.00	−3.08	1.03			
25.17	−3.16	1.13	33.80	−1.69	1.39	45.10	−6.09	−0.04	53.11	−3.28	0.92			
25.48	−2.27	1.44	34.22	−2.17	1.29	45.38	−2.43	1.29	53.30	−3.83	0.76			
25.64	−2.19	1.32	34.53	−1.88	1.38	46.00	−2.62	1.04	53.64	−3.44	0.82			

BGD
10, 7989–8025, 2013

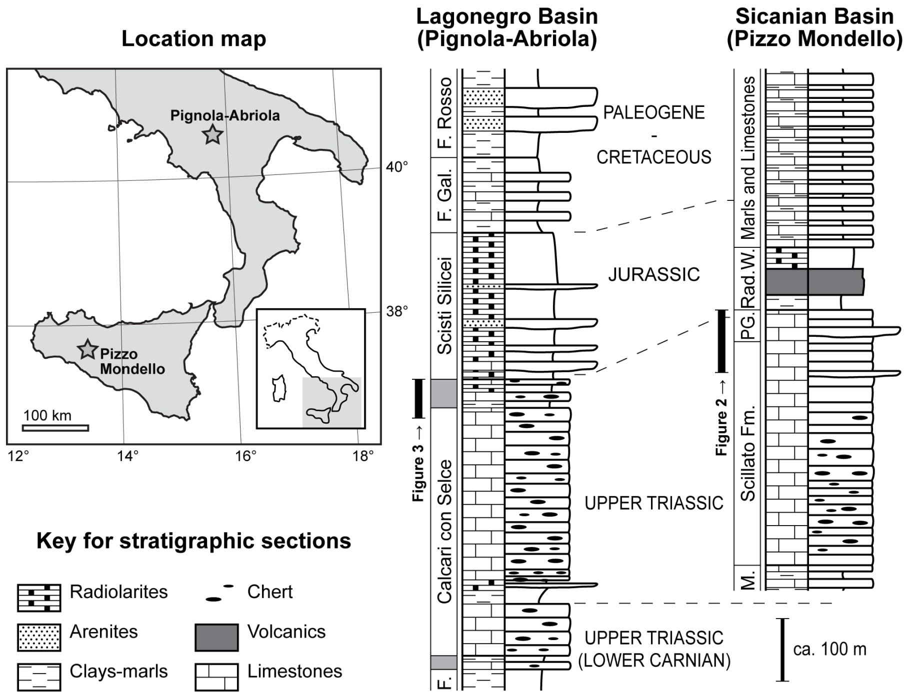

Fig. 1. Location of the studied stratigraphic sections in Southern Italy, and synthetic stratigraphic succession of the Lagonegro Basin at Pignola (modified from Passeri et al., 2005) and of the Sicanian Basin at Pizzo Mondello (modified from Di Stefano et al., 1996). The scale is approximated.

BGD
10, 7989–8025, 2013

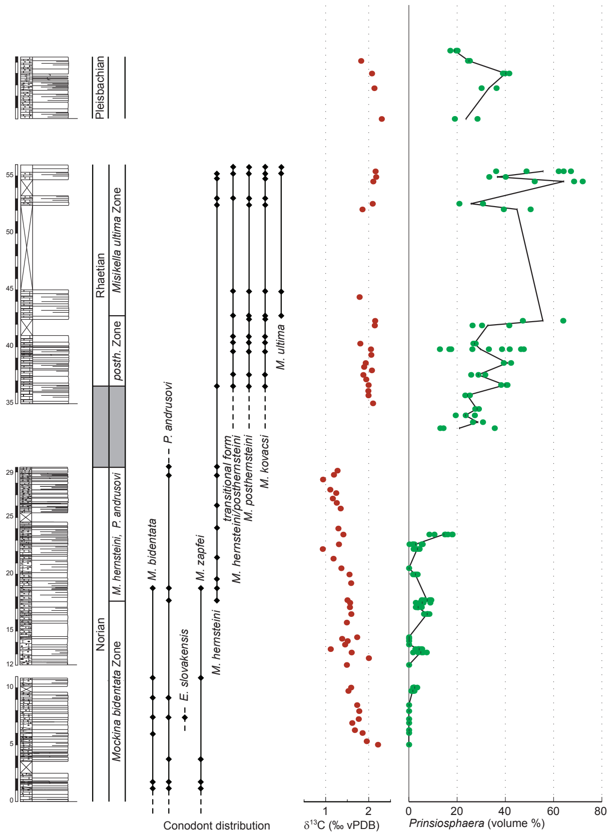

Fig. 2. Stratigraphy, stable carbon isotopes from bulk carbonate and volume proportion of calcareous nannofossils at Pizzo Mondello (Sicanian Basin, Sicily). The black line connects mean volume proportions of nannofossils. Biostratigraphy from Mazza et al. (2012) and Preto et al. (2012). Conodont biozones according to Kozur and Mock (1991). Lithological symbols as in Fig. 1.

BGD
10, 7989–8025, 2013

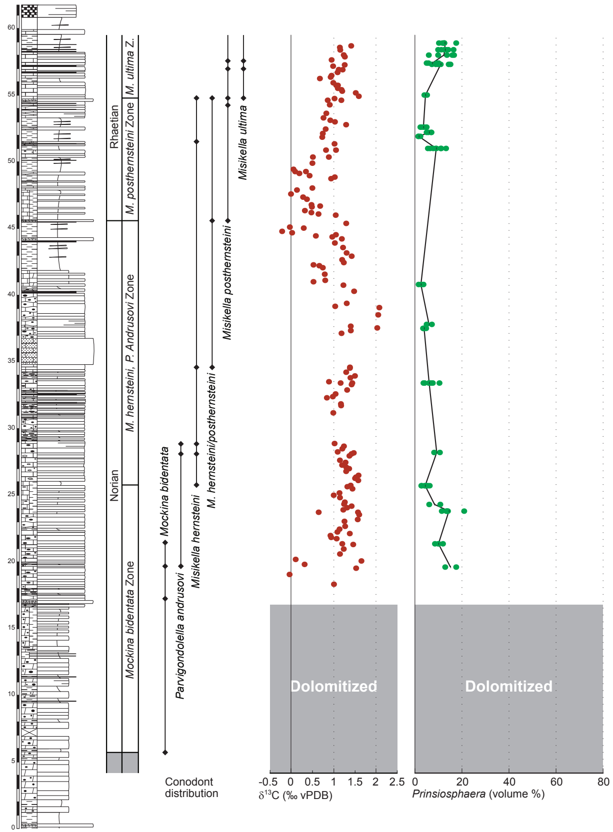

Fig. 3. Stratigraphy, stable carbon isotopes from bulk carbonate and volume proportion of calcareous nannofossils at Pignola–Abriola (Lagonegro Basin, Southern Apennines, Southern Italy). The black line connects mean volume proportions of nannofossils. Conodont distribution and biozones from Giordano et al. (2010). Conodont biozones according to Kozur and Mock (1991). Lithological symbols as in Fig. 1.

BGD
10, 7989–8025, 2013

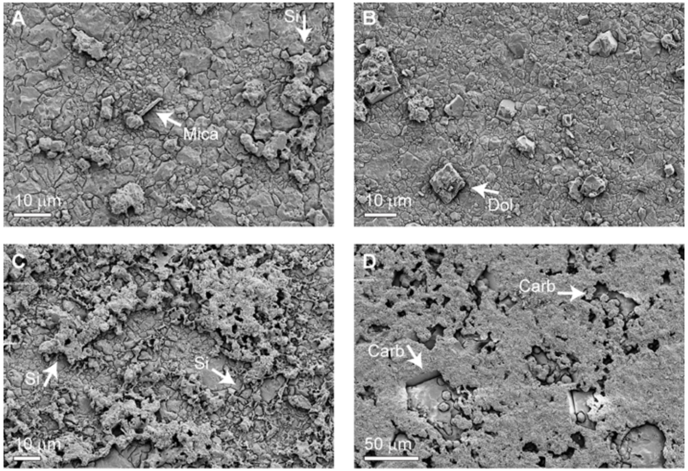

Fig. 4. Examples of diagenetic alteration of micrite and microsparite. **(A)** Slightly silicified sample with minor terrigenous component (mica crystal in the center of the frame). Calcareous nannofossils are easily visible. Silicified plagues (Si) stick out of the sample plain because of etching. Pignola–Abriola section, *Paragondolella andrusovi* – *Misikella hernsteini* conodont zone, late Norian, 33.3 m in Fig. 3. **(B)** Dolomite rhombohedrons (Dol) in microsparitic lime mudstone. Pignola–Abriola section, *Misikella ultima* conodont zone, Rhaetian, 58.8 m in Fig. 3. **(C)** Silicified lime mudstone. Silica (Si) occupies a large part of the rock volume in this frame, and can be found in interstitial position between carbonate crystals or as plagues. Pignola–Abriola section, *Paragondolella andrusovi*–*Misikella hernsteini* conodont zone, late Norian, 40.7 m in Fig. 3. **(D)** Strongly silicified sample. Carbonate (Carb) is only present as a few crystals, that partially engulf silica with spheroidal shape (chalcedony?). Locally, carbonate crystal faces are instead preserved. Pignola–Abriola section, *Paragondolella andrusovi* – *Misikella hernsteini* conodont zone, late Norian, 45.1 m in Fig. 3.

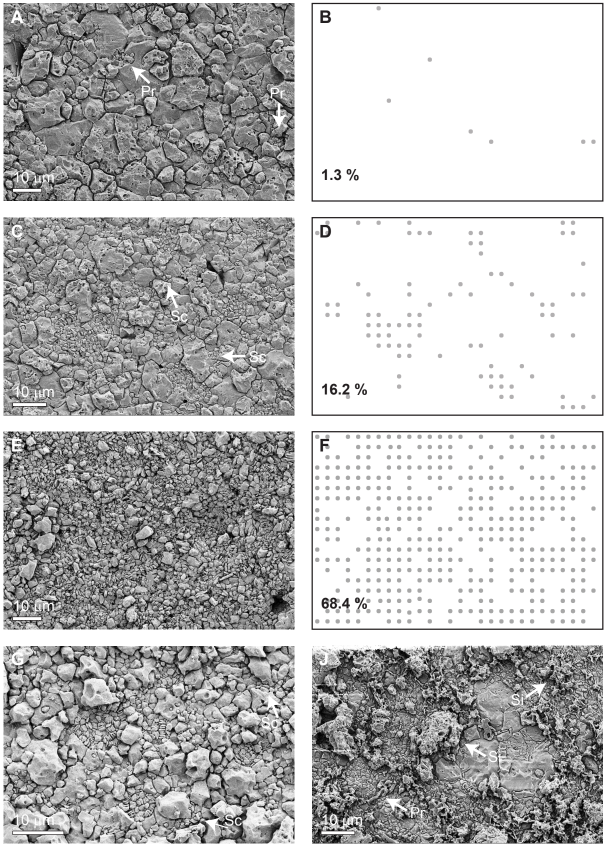

Fig. 5. Caption on next page.

BGD
10, 7989–8025, 2013

The calcareous nannofossil *Prinsiosphaera*

N. Preto et al.

Title Page
Abstract Introduction
Conclusions References
Tables Figures
◀▌ ▌▶
◀ ▶
Back Close
Full Screen / Esc
Printer-friendly Version
Interactive Discussion

Fig. 5. Microfacies of late Norian and Rhaetian lime mudstones from Pignola–Abriola and Pizzo Mondello, as seen under the SEM. All samples of this figure were prepared with polishing and etching. In **(A–E)**, SEM images are compared with the results of point counting. Three examples, with scarce, abundant and dominant *Prinsiosphaera* are shown. **(A, B)** Sample from the *Mockina bidentata* conodont zone, late Norian of Pizzo Mondello, 9.71 m in Fig. 2. Note large microspar crystals with pits highlighted by etching. Pr = *Prinsiosphaera*. **(C, D)** Sample from the *Paragondolella andrusovi–Misikella hernsteini* conodont zone, late Norian of Pizzo Mondello, 23.74 m in Fig. 2. In this sample, complete specimens of *Prinsiosphaera* are associated with isolated scales (Sc) of disaggregated *Prinsiosphaera* "calcispheres". **(E, F)** Sample from the *Misikella ultima* conodont zone, Rhaetian of Pizzo Mondello, 54.5 m in Fig. 2. *Prinsiosphaera* is here the dominant rock component. Single specimens are compacted and indistinguishable. Note the fine microspar, with crystals always smaller than 10 µm. **(G)** Sample from the *Mockina bidentata* conodont zone, late Norian of Pignola–Abriola, 23.7 m in Fig. 3. Complete specimens of *Prinsiosphaera* with well developed piles of scales are here associated with isolated scales (Sc), often engulfed by the surrounding microspar. **(J)** Sample from the *Misikella posthernsteini* conodont zone, Rhaetian of Pignola–Abriola, 52.1 m in Fig. 3. Silicization formed in this sample plagues of amorphous silica or chert (Si) in interstitial positions, that stick out of the sample surface after etching. The large, subrounded plague in the center may be a substituted radiolarian test. *Prinsiosphaera* (Pr) are still well recognizable and some microspar is also observed.

BGD
10, 7989–8025, 2013

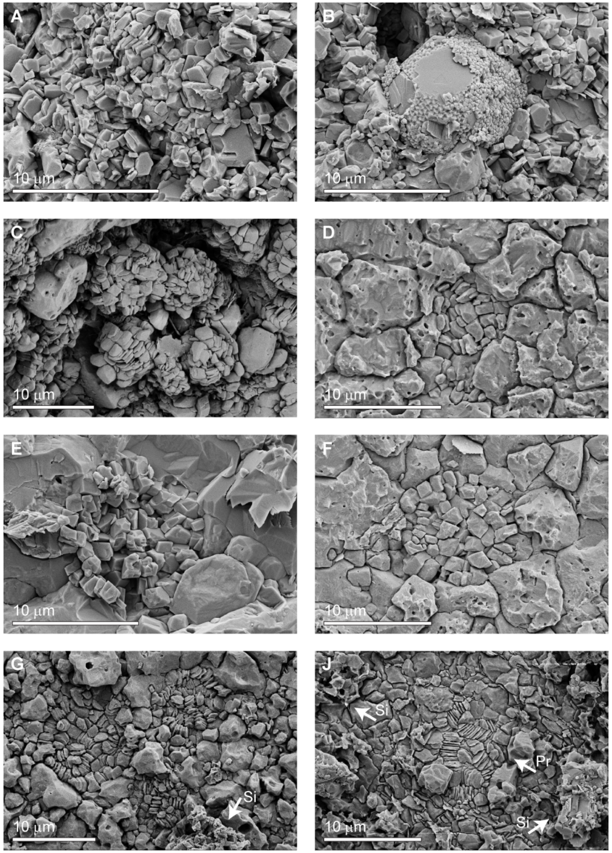

Fig. 6. Caption on next page.

BGD
10, 7989–8025, 2013

Fig. 6. Calcareous nannofossils from the Late Norian and Rhaetian of the Southern Apennines and Sicily. **(A)** Scales of *Prinsiosphaera* from the *Misikella ultima* conodont zone, Rhaetian of Pizzo Mondello, 54.5 m in Fig. 2; fresh broken sample. In this example, *Prinsiosphaera* "calcispheres" cannot be discerned either because they were disarticulated, or because they have been compacted during burial. **(B)** *Thoracosphaera geometrica* from the *Misikella ultima* conodont zone, Rhaetian of Pizzo Mondello, 54.5 m in Fig. 2; fresh broken sample. This and other nannofossils, different from *Prinsiosphaera*, are minor constituents of the carbonate sediment at Pizzo Mondello and were not recognized at Pignola–Abriola. **(C)** *Prinsiosphaera* from the *Misikella posthernsteini* conodont zone, Rhaetian of Pizzo Mondello, 40.25 m in Fig. 2; surface of "calcispheres" within a primary cavity of the sediment. **(D)** *Prinsiosphaera* from the *Paragondolella andrusovi–Misikella hernsteini* conodont zone, Late Norian of Pizzo Mondello, 19.95 m in Fig. 2; polished and etched sample. **(E, F)** *Prinsiosphaera* from the *Mockina bidentata* conodont zone, late Norian of Pizzo Mondello, 13.1 m in Fig. 2; comparison of the freshly broken sample **(E)** and polished and etched sample **(F)**. **(G)** Three specimens of *Prinsiosphaera* with different diameters from the *Mockina bidentata* conodont zone, late Norian of Pignola–Abriola, 23.7 m in Fig. 3. This sample was polished and etched. Silicification (Si) is visible. **(J)** *Prinsiosphaera* (Pr) and silicified plagues (Si) from the *Misikella posthernsteini* conodont zone, Rhaetian of Pignola–Abriola, 52.1 m in Fig. 3. Polished and etched sample.

BGD
10, 7989–8025, 2013

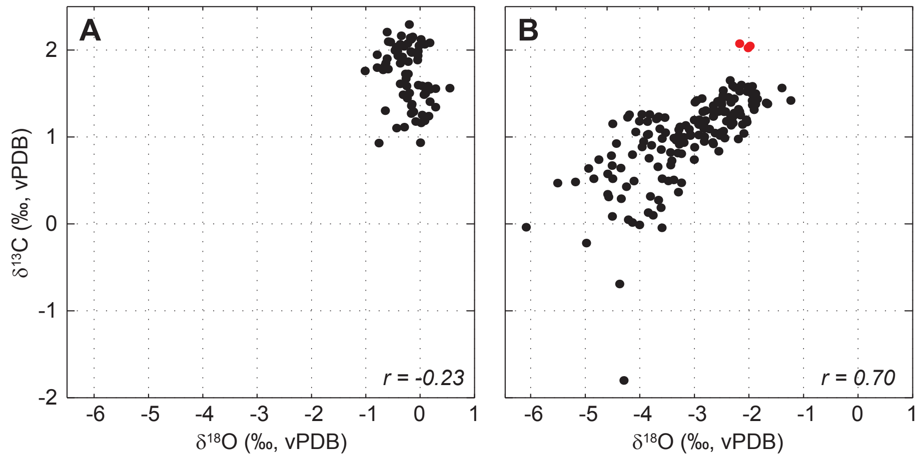

Fig. 7. Crossplots of stable isotope analyses of bulk carbonate from **(A)** Pizzo Mondello and **(B)** Pignola–Abriola. The samples marked in red are from a thick calciturbidite in the uppermost Norian portion of the Pignola–Abriola section. Correlation coefficients (*r*) are both significantly different from zero.

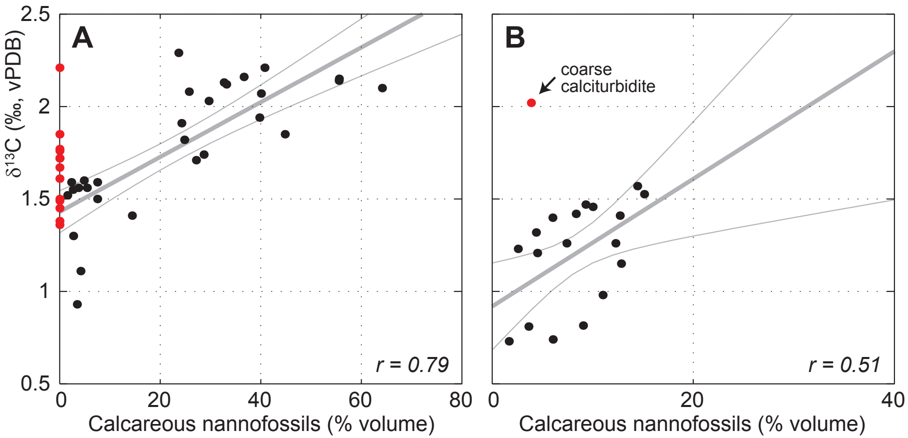

Fig. 8. Carbon isotope composition (δ^{13}C) of lime mudstone plotted against the abundance of calcareous nannofossils at Pizzo Mondello **(A)** and Pignola–Abriola **(B)**. The δ^{13}C is clearly correlated with nannofossil abundance, see correlation coefficients (r). Linear fit is plotted with 90 % error bounds. Twelve samples of Pizzo Mondello without nannofossils, and one sample of Pignola from a 2 m thick coarse calciturbidite are marked in red and were excluded from computation.

BGD
10, 7989–8025, 2013

Title Page
Abstract Introduction
Conclusions References
Tables Figures
◀ ▶
Back Close
Full Screen / Esc
Printer-friendly Version
Interactive Discussion

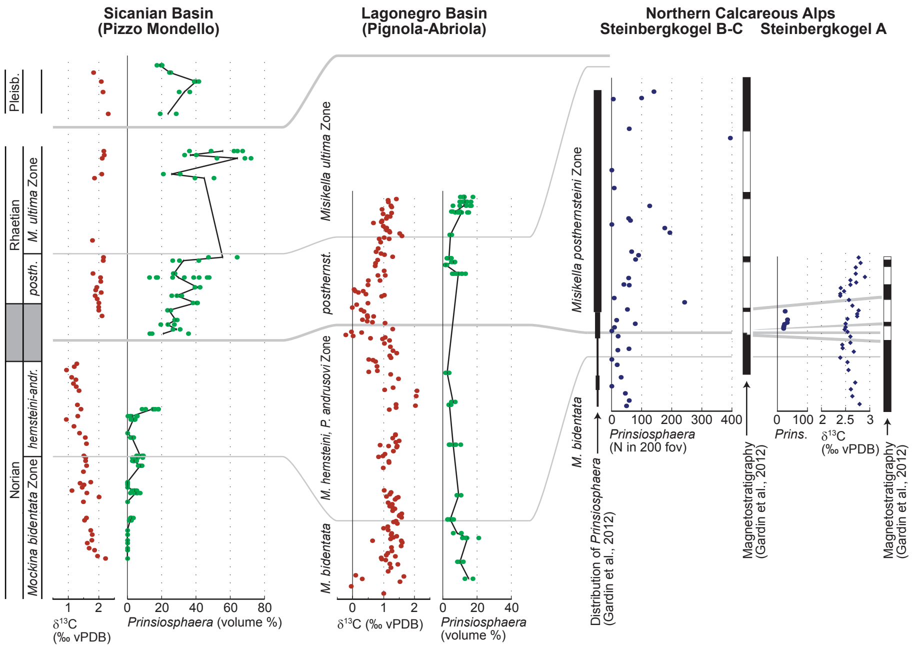

Fig. 9. Correlation of isotopic and nannofossil records between Pizzo Mondello, Pignola–Abriola and Steinbergkogel (Gardin et al., 2012). The correlation with Steinbergkogel is only based on conodont biostratigraphy, and it could thus be inaccurate as highlighted by Giordano et al. (2010). Distribution of *Prinsiosphaera* and magnetostratigraphy at Steinbergkogel are reported as in Gardin et al. (2012). Blue dots are obtained from Table 4 in Gardin et al. (2012). Stable carbon isotopes from Krystyn et al. (2007). FOV: Fields of view.

BGD
10, 7989–8025, 2013

The calcareous nannofossil *Prinsiosphaera*

N. Preto et al.